Seasonal rockfall risk analysis in a touristic island: Application to the Tramuntana Range (Mallorca, Spain)

Pedro Pinto Santos [a, *], Cristina Reyes-Carmona [b], Susana Pereira [a, c], Roberto Sarro [d], Mónica Martínez-Corbella [d], Miquel Àngel Coll-Ramis [e], José Luís Zêzere [a], Rosa María Mateos [d]

[a] *Centre of Geographical Studies, TERRA Associate Laboratory, Institute of Geography and Spatial Planning, University of Lisbon, Rua Branca Edmée Marques, 1600-276, Lisboa, Portugal*
[b] *Department of Civil Engineering, Escuela Politécnica Superior, University of Alicante, Carrer de San Vicente del Raspeig, 03690, San Vicente del Raspeig, Alicante, Spain*
[c] *Centre of Studies in Geography and Spatial Planning, Geography Department, Faculty of Arts and Humanities, University of Porto, Via Panorâmica s/n, 4150-564, Porto, Portugal*
[d] *Department of Geohazards and Climate Change, National Centre Geological and Mining Institute of Spain (IGME-CSIC), Ríos Rosas 23, 28003 Madrid, Spain*
[e] *Department of Geography, Universitat de les Illes Balears, Carretera de Valldemossa km 7.5, 07122, Palma, Mallorca, Balearic Islands, Spain*

ARTICLE INFO

ABSTRACT

Rockfalls are an ever-present possibility in the mountainous context of the Tramuntana Region (Mallorca, Spain). Recent events have shown the high potential for direct and indirect impact on the safety of people and economic activities, lasting for weeks or even months. In the present study, we start from a probabilistic assessment of the rockfall hazard (spatial propensity and temporal recurrence), based on a detailed historical record of occurrences and rockfall modelling, which is subsequently superimposed on three exposure scenarios and on a social vulnerability assessment. Exposure considers the floating population at three seasons of the year, given the area's high tourist aptitude. Vulnerability considers on the one hand the intrinsic characteristics of individuals and, on the other, the characteristics of the surrounding territory that act to facilitate emergency operations, mitigate the immediate impact and enhance rapid recovery. Due to the characteristics of the island and the spatial distribution of tourism, the results show that the highest density of rockfall trajectories potentially affect areas of high exposure, whose access by emergency services is complex. Not being, in general, the areas of highest individual criticality, those areas have in most situations low support capability installed or nearby.

The results constitute a useful tool for emergency and risk management planning in multiple sectors linked to risk governance. Despite the high geographic detail of the analysis, these studies do not replace exposure and vulnerability analysis at the building level, for which the contribution of georeferenced Census data is fundamental.

* Corresponding author.
E-mail address: pmpsantos@campus.ul.pt (P.P. Santos).

1. Introduction

In the tourism industry, safety plays a critical role in determining travel decisions. Destinations that are perceived to be unsafe experience a significant decrease in the number of visitors, which can have a devastating effect on the local economy [1,2].

Hazards in tourist destinations, especially on islands, must be known to better understand and manage tourism vulnerability to natural hazards [3]. Those islands face challenges in the hazards and vulnerability assessments, including biased estimations of human exposure and social vulnerability due to the seasonal inflow of tourists, and increasing in the foreign-born population [3].

To effectively respond to and recover from disasters related to geohazard events like earthquakes, landslides, volcano eruptions, tsunamis, and floods, it is essential to address the risk perceptions and behaviors of tourism stakeholders. This includes developing risk management strategies that aim to reduce the impact of potential hazards on the tourism industry, such as emergency planning, crisis communication, and risk assessment. Through effective engagement with stakeholders, tourism managers can successfully manage risks and bolster the resilience of their destination [4,5].

Rockfalls are a frequent and dangerous type of slope instability process and consequently they have a great socioeconomic impact throughout the world [6]. These slope movements are defined as a sudden and high-velocity mass movement, where at least part of the displacement involves free fall [7]. Although rockfalls may not mobilize large volumes of material, they can be extremely destructive due to two main factors: the high velocities that blocks can reach during their fall, making it difficult to respond rapidly, and the unpredictability of when these events will occur. Rockfall occurrences worldwide are not a result of random processes but rather they are influenced by a complex interplay of geological, geomorphological, and environmental factors. Weather patterns, particularly heavy rainfall and abrupt temperature changes are the primary triggers of such events.

In rockfall risk management – thinking not only in the emergency and contingency operations, but in the preventive measures as well – the hazard component of the assessment should take into account both, i) the location and characteristics of the main source areas of rockfall movement and ii) the trajectory and projection areas of the displaced blocks (e.g. Ref. [8]. Modelling rockfall hazard is a high-complexity task due to several factors: limited temporal recurrence, short permanence of post-event traces or poor availability of conditioning factors' data [9]. An additional difficulty to be mentioned is producing and updating a rockfall database or inventory with precise information about location, date and magnitude of each rockfall event. In this sense, the availability of an inventory as complete as possible is the starting point to manage hazard, what usually involves great efforts in searching and compiling this kind of data. The exposure is a fundamental risk component in explaining the degree of observed losses due to natural hazards, including landslides and rockfall processes [10–13]. The estimation of the population exposure, especially in touristic areas, such as Mallorca Island, is a very challenging task due to the high mobility, high range of daily activities and seasonal characteristics of the tourists. Frequently, in comparison with the local population, tourists are more vulnerable in disaster situations justified by its less informed perceptions of local hazard, less independence resulting from the absence of a familiar environment and can have language barriers which can result in risks underestimation [14,15]. The understanding of the social vulnerability factors is mandatory to contribute to risk reduction and mitigation measures and safer tourism destinations. Social vulnerability is dynamic and reflects complex social relations, mobility, community cohesion, demography, gender, age, educational level, health status, foreign population, and foreign languages [16]. Regarding the assessment of social vulnerability specifically to the rockfall hazard in tourist areas, existing studies are limited. In Ref. [17]; the presence of tourists was considered a fundamental factor, with different degrees of loss assumed depending on the context of mobility of the exposed individuals. [18]; delving into a methodology by Ref. [19]; separately consider the social vulnerability of individuals based on their location in buildings or along the road network. In this score-based index, they took into account social worth, time of stay (hours per day), and the value of the exposed element, assuming that the assignment of values should always be done on a case-by-case basis. Scientific research that proceeds with the transfer of methodologies for assessing SV from one type of hazard to another – that shares characteristics explaining the potential loss – is revealed as fundamental [20].

A preliminary study of social vulnerability analysis to natural disasters at the municipal level of the Mallorca Island [16] was based on a multicriteria analysis to weight the social vulnerability factors based on an expert-based questionnaire. In this study, the following vulnerability factors were used: demographic and social, economic and access to infrastructure and services. In general, it was not detected significant changes in social vulnerability at the municipal level and there is a high level of wealth and territorial equilibrium [16].

The exponential growth of population (local and foreign-born) and the intensification of land-use and second home tourism in peri-urban areas have led to an increase in the risk of rockfalls. This issue requires a deeper understanding that foster effective solutions through the implementation of protocols, methodologies, and advanced tools for rockfall risk management.

In this paper, we present a rockfall risk analysis performed at the census section-scale in the Tramuntana region (Mallorca Island). The main objectives of this study are the following: (i) to assess a probabilistic rockfall hazard (spatial, temporal and magnitude probability); (ii) to assess population exposure, considering resident population and three scenarios of floating population associated with tourism (low, medium and high exposure scenarios), over the year; (iii) to assess social vulnerability of the resident population; and (iv) to compute rockfall risk and discuss its usefulness in risk management in the study area.

2. Study area

The Serra de Tramuntana region (Mallorca, Spain) is morphologically defined by a mountainous NE-SW alignment with a maximum length of 90 km and an average width of 15 km of homonymous denomination (the Tramuntana Range) (Fig. 1A).

The lithology is dominated by limestones and dolostones dating from the Jurassic (Fig. 1B), that constitute the highest relief massifs by many NW-overlapping thrusts linked to the Alpine orogeny [49]. The older underlying materials are mainly Late Triassic clays and gypsums (Fig. 1B), that act as the regional basal detachment of the thrust system and outcrop in the SW sector of the region. More
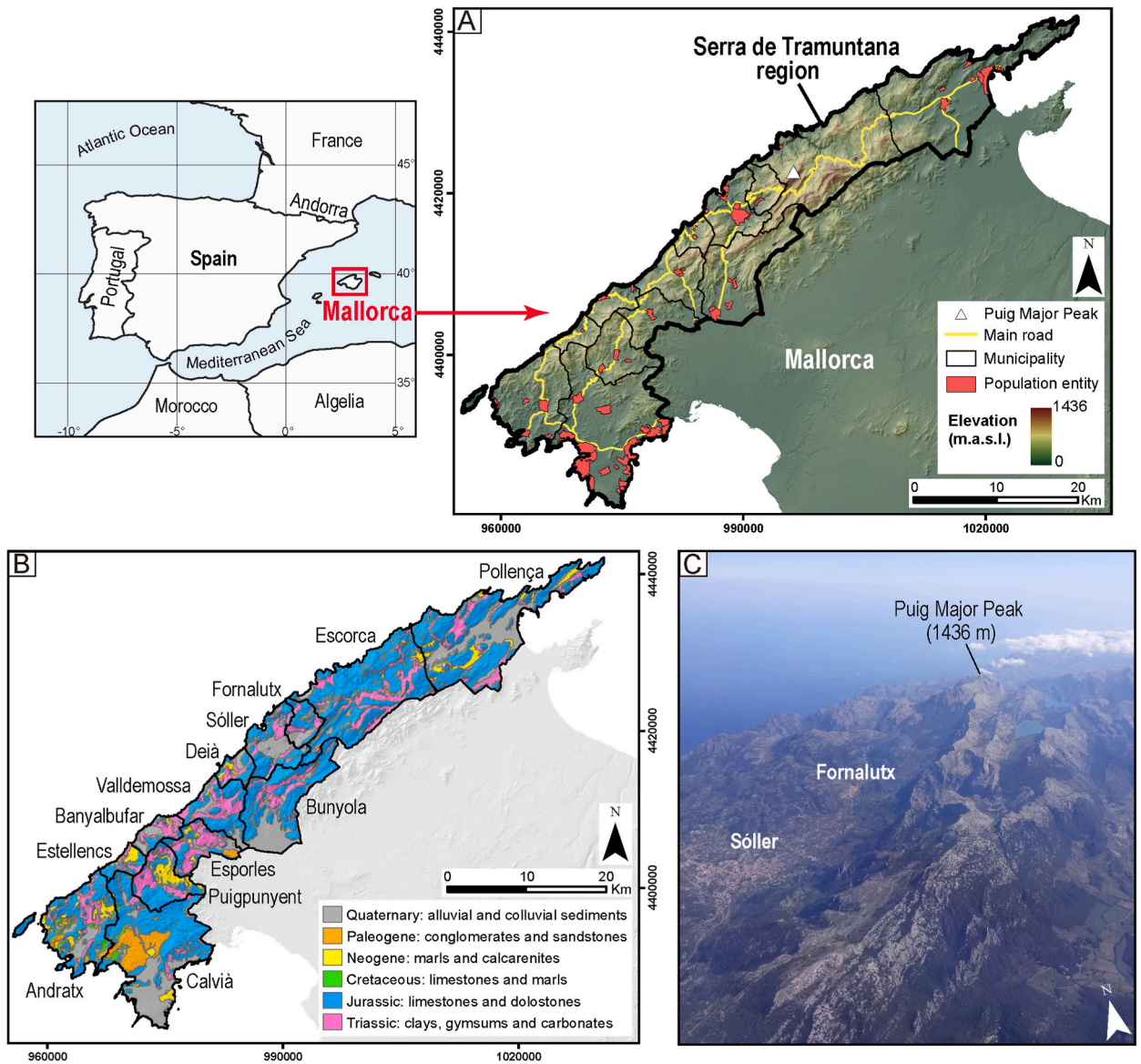
Fig. 1. Geographical context (A) and lithological map (B) of the Serra de Tramuntana region on the island of Mallorca; (C) panoramic view of the highest Jurassic limestones reliefs in the Serra de Tramuntana mountain range.

recent Plio-Quaternary colluvial and alluvial sediments are found in the SE strip of the region (Fig. 1B) [21]. The presence of steep slopes, a favorable lithology to slope instability and high density of faults and discontinuities – subjected to high variations in temperature and moisture conditions along the day and accentuated by the pluviogenic effect of the mountain range – leads to classifying the study area as highly susceptible to slope movements (Mateos et al., 2012, [9]. According to Ref. [22]; 70 % of the reported mass-movement events (almost 900 since the eighteenth century) correspond to rockfalls, which are mainly originated in the Jurassic limestones.

The rockfall average volume is 600 m^3, ranging from small cobbles to large blocks of hundreds/thousands of cubic meters. Many damaging rockfall events have been recently recorded in the Tramuntana region, such as the one in Banyalbufar, in 1993, or in Valldemossa, in 2005, that affected fishing huts and archeological sites, respectively [23,24]. During 2008 and 2010, an extraordinary cold and wet winter occurred on the island of Mallorca, resulting in daily rainfall values of up to 300 mm, annual accumulated rainfall that doubled the average [9] and freezing processes in the Tramuntana range [50]. These climatic conditions triggered 15 rockfalls with no fatalities but caused several damages to dwellings, power stations, and the road network. Specifically, the Ma-10 road, the main transportation route connecting all the municipalities of the Serra de Tramuntana region, was seriously affected by events such as the Gorg Blau rockfall in the municipality of Escorca [9]. With a volume of 30,000 m^3, this event occurred in December 2008 and blocked the Ma-10 road for three and a half months, resulting in repair costs of 1.8 million Euro and indirect costs of 1 million Euro [26].

This Alpine chain was declared World Heritage Site in 2011, a status that contributed even more to emphasizing the touristic vocation of the study area, combining mountain and coastal leisure, cultural, historical and sports activities. The study area has 834.16 km², and is statistically subdivided into 59 census sections, grouped in the 13 municipalities of the Tramuntana region. The resident population has been increasing in the last decades, with the main contribution of immigration and foreign-born population and the economic activities associated with tourism. The resident population is of 108,220 people – with the municipality of Calvià representing almost half of that sum (49,675 people) in 2011 population Census –, to which a floating population estimated in 75,399 persons in the high touristic season alone [27,28]. Between June and October almost 8,000,000 tourists were recorded in 2022 in Mallorca [27], which 85.6 % were from foreign countries, increasing the potential number of victims, as they are unaware of the risks they face while in holidays and Spanish is not their mother tongue. Rapid urban development in the region in the last 30 years has increased the exposure to several hazards including general-landslide movements [21,25], droughts and flash floods [29]. However, it needs to be considered that the new inhabitants do not know the territory and are unaware of the major damaging hazards present on the island.

3. Data and methods

Fig. 2 represents a simplified methodological flowchart of the rockfall risk performed at the census sections of the Serra de Tramuntana region. Although the final risk index is represented at the census section level, the geographical representation of several data sources and intermediate layers of information follows other units of representation. This is particularly valid for the hazard and the support capability components of risk, which use pixel- and vector-format data, respectively. Criticality input data was already represented at the census section level. Each of the risk components will be described in detail in the following sections, including the input data, its processing and transformation into the census section level.

3.1. Rockfall hazard

Rockfall hazard (*H*) results from the following equation (Eq. (1)):

$$H = P(S) * P(T) * P(M) \tag{Eq. 1}$$

where, *P(S)* and *P(T)* are respectively the spatial and temporal probability of a rockfall, and *P(M)* is the probability of occurrence of a rockfall with a given magnitude.

For the case study of the Tramuntana Range, the final rockfall hazard map is represented by means of a GIS in normalized values from 0 (minimum hazard) to 1 (maximum hazard). Four hazard categories have been established, according to the standard deviation (SD) of the data, as follows: low (<0.5 SD), moderate (0.5–1.5 SD), high (1.5–2.5 SD) and very high (>2.5 SD).

In the following subsections, the steps for the calculation of these hazard components are presented.

3.1.1. Spatial probability

For the calculation of spatial probability or susceptibility *P(S)*, a raster map of simulated rockfall trajectories was used (Fig. 3A). This raster was obtained using STONE, a 3-dimensional software that relies on physically based simulations [30]. As mainly input files (in.tif format), the software requires: (1) a Digital Elevation Model (DEM); (2) the location of the rockfall source areas; and (3) three coefficients of the involved rocks that simulate energy loss when rock blocks roll and bounce at impact points, which are based
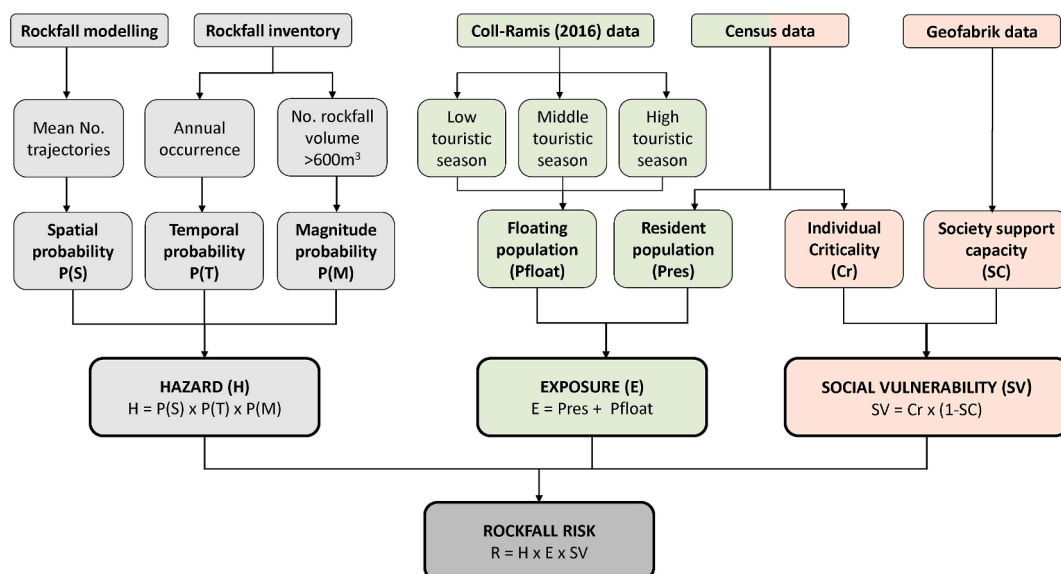

Fig. 2. Methodological flowchart of the rockfall risk analysis in Tramuntana region.
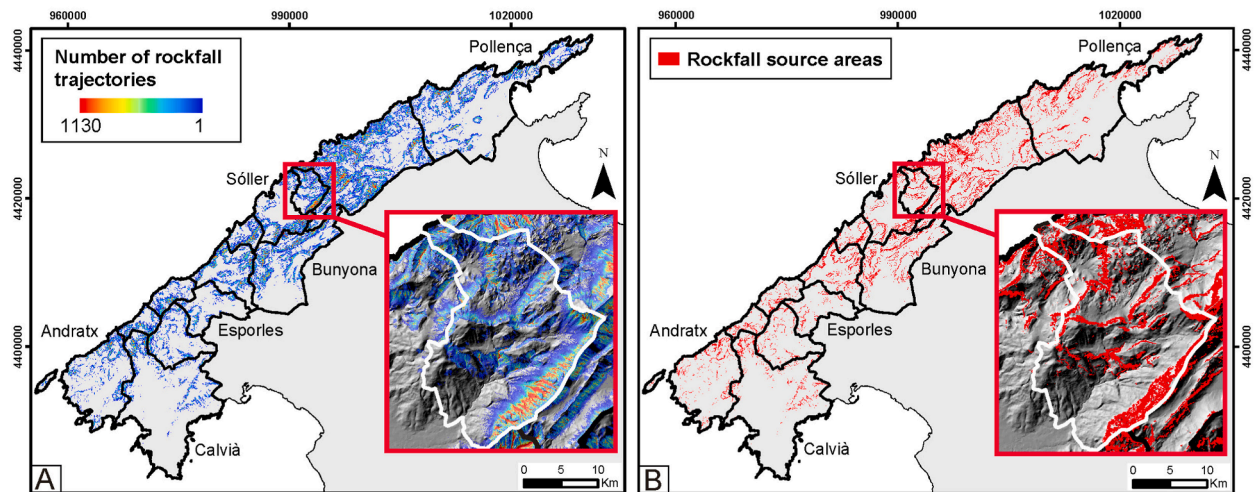
Fig. 3. Simulated rockfall trajectories obtained from the software STONE (A) and source areas used for the rockfall simulation (B), including a zoomed-in view of both maps in the Fornalutx municipality.

on the dynamic rolling friction, normal energy restitution, and tangential energy restitution. The software simulates a series of rockfall trajectories and produces a raster map showing the number of trajectories for each pixel (Fig. 3A).

In our modelling, we used a DEM of 10 m resolution, provided by the National Centre for Geographical Information (CNIG; https://centrodedescargas.cnig.es/CentroDescargas/index.jsp).

The values of the dynamic rolling friction, the normal and the tangential energy restitution coefficients were obtained from the geotechnical map of the Serra de Tramuntana [9]. These coefficients, based on the simple compressive strength of the materials, classify the strength of the different lithologies (Fig. 1B) into five categories: hard rocks, moderately hard rocks, soft rocks, soft soils, and very soft soils. These coefficient values were also coherently selected according to previous works of rockfall modelling in the Tramuntana Range [8,9].

Rockfall source areas (Fig. 3B) were identified according to the criteria proposed by Ref. [9]; which are based on topographic and geological data. In this way, source areas were defined as slopes with an angle exceeding 35° and composed of hard or moderately hard rocks (Fig. 3B). Due to the socio-economic significance of the coastal region in the Serra de Tramuntana and its distinctive topographical features, including a dynamic shoreline with steep cliffs and sandy beaches, source areas were also established within legally protected areas, such as the Terrestrial Marine Public Domain (DPMT), and within 100 m of Private Domain Protection.

For each source area pixel were performed 5 simulations. The final calculation of *P(S)* for each census section was made by the product of the mean number of rockfall trajectories in the section ($no.Traj_{mean}$) and the coefficient between the rockfall susceptible area (A_{rs}) and the total census section area (A_{cs}), in km². The rockfall susceptible area (A_{rs}) is referred to the area that comprise any trajectory value, from 1 to 1130 (Fig. 3A). Thus, the proposed equation would be (Eq. (2)):

$$P(S) = no.\,Traj_{mean} * \left(A_{rs}/A_{cs} \right) \tag{Eq. 2}$$

Finally, the obtained spatial probability values were normalized and spatially represented for each census section in a GIS through four classes that were defined according to the standard deviation (SD) of the data, as follows: low (< -0.5 SD), moderate (−0.5 to 0.5 SD), high (0.5–1.5 SD) and very high (>1.5 SD).

3.1.2. Temporal probability

For the calculation of the temporal probability *P(T)*, the information was derived from a rockfall inventory that compiles events documented in previous works [9,22]; together with new events reported by the General Directorate of Emergencies of the Government of the Balearic Islands and the Council Road Service from the Island of Mallorca. This new inventory is updated to 2020 and it contains a total of 832 rockfall events (Fig. 4A). Only 364 of these events content information about the date they occurred (Fig. 4B), between 2005 and 2020 (16 years), which were selected for the *P(T)* calculation. In each census section, the number of these events (*no.events*) was obtained and divided by the area of the section (A_{cs}), in km², for thus obtaining a density of rockfalls. This density was then divided by *16* (the number of years in the recorded inventory) to obtain an annual probability for this time interval. Thus, the proposed equation would be (Eq. (3)):

$$P(T) = \left(no.\,events/A_{cs} \right) /16 \tag{Eq. 3}$$

Finally, the obtained temporal probability values were normalized and spatially represented for each census section in a GIS through four classes that were defined according to the standard deviation (SD) of the data, as follows: low (< -0.5 SD), moderate (−0.5 to 0.5 SD), high (0.5–1.5 SD) and very high (>1.5 SD).
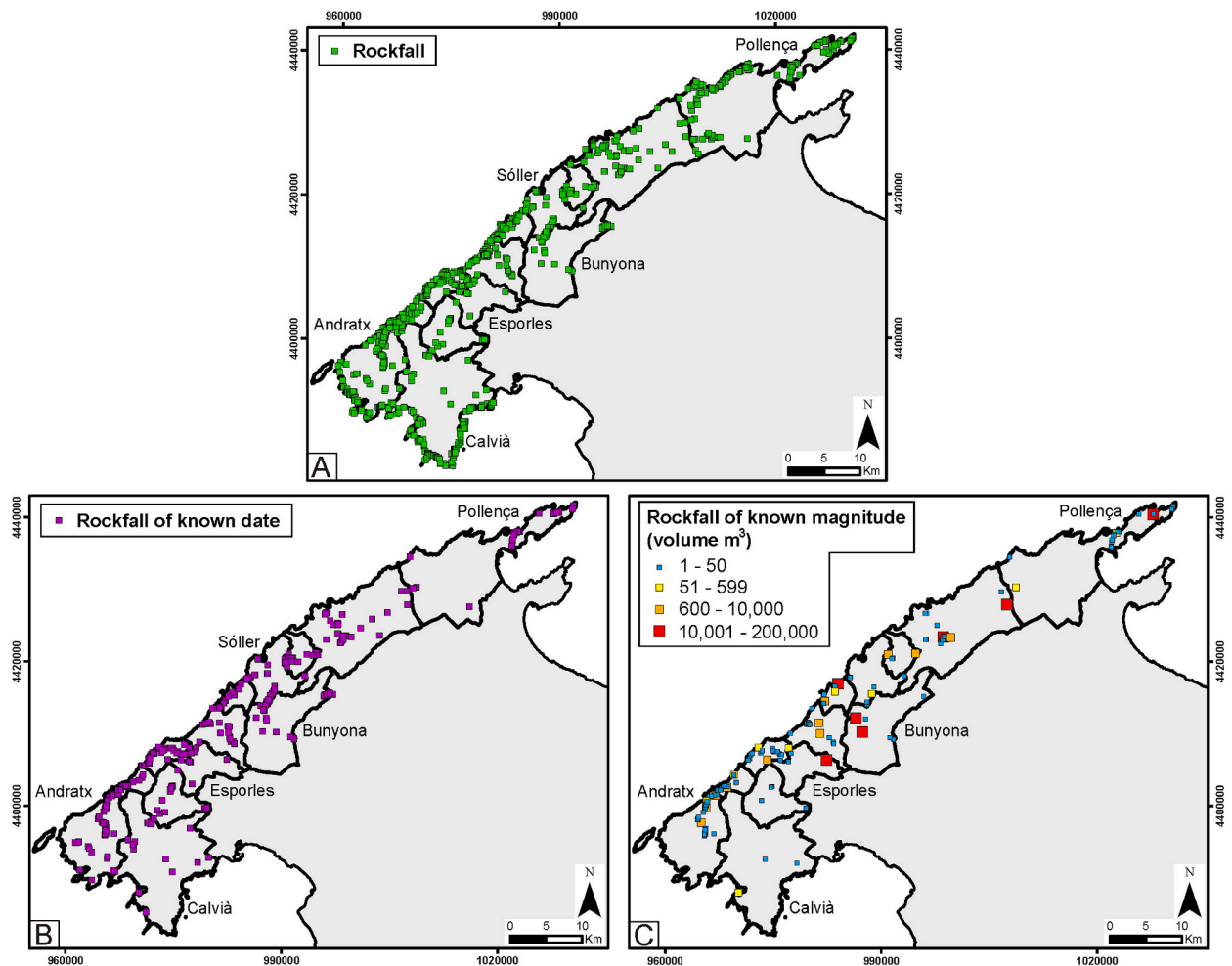
Fig. 4. Rockfall inventory updated to 2020 (A); rockfall events of known date (B) and known magnitude given in volume (C) extracted from the inventory of Fig. 4A.

3.1.3. Magnitude probability

From the newly updated inventory (Fig. 4A), only 162 rockfalls events contain information about their magnitude, which is given in volume (m^3) (Fig. 4C). To calculate the probability of rockfall occurrence based on their magnitude *P(M)*, rockfalls with a volume greater than 600 m^3 were selected, with 200,000 m^3 being the maximum recorded volume. Only 18 events that meet this criterion out of the 162 (Fig. 4C). The volume threshold of 600 m^3 was established by using a geometric intervals' classification of the data, which works best for very scattered data spread over a large area. Moreover, the value of 600 m^3 coincides with the average volume value from previous studies [22]. The purpose of selecting this threshold was to capture only the larger magnitude and potentially more destructive rockfall events, despite their lower frequency. Thus, the *P(M)* calculation was defined according to the number of events (0, 1, 2 or 3) larger than 600 m^3 for each census section and were then normalized, ranging from minimum (0) to maximum probability (1). The data was spatially represented according to its standard deviation (SD) in the following classes: low (<0.5 SD), moderate (0.5–1.5 SD), high (1.5–2.5 SD) and very high (>2.5 SD).

3.2. Exposure

Exposure (*E*) refers to the elements exposed to rockfalls, which in the Tramuntana Range included only the exposed population. The novelty included in this calculation is that it considers not only the resident population *(Pres)* recorded in the 2011 INE census, but also the floating population *(Pfloat)* associated with tourist seasons (Fig. 5).

Therefore, three scenarios of exposed population have been obtained according to the three existing tourist seasons: low (November, December, January and February), middle (March, April, May and October) and high (June, July, August and September).

The floating population was estimated from the total number of tourist accommodations per municipality multiplied by the occupancy rate in each season, following the method proposed by Ref. [31]. Based on this information, a downscaling of floating population exposure to the census section level was performed for each touristic season scenario. The floating population data considered at the municipal level have been taken to subsequently carry out an equitable distribution in proportion to the census population of each block, using the following equation (Eq. (4)):
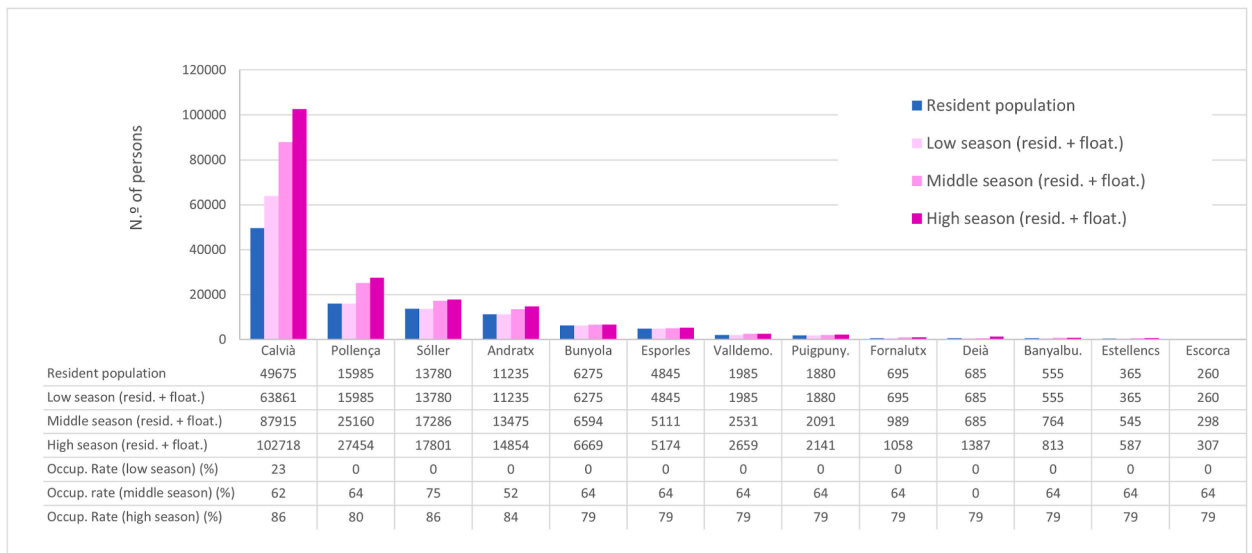
	Calvià	Pollença	Sóller	Andratx	Bunyola	Esporles	Valldemo.	Puigpuny.	Fornalutx	Deià	Banyalbu.	Estellencs	Escorca
Resident population	49675	15985	13780	11235	6275	4845	1985	1880	695	685	555	365	260
Low season (resid. + float.)	63861	15985	13780	11235	6275	4845	1985	1880	695	685	555	365	260
Middle season (resid. + float.)	87915	25160	17286	13475	6594	5111	2531	2091	989	685	764	545	298
High season (resid. + float.)	102718	27454	17801	14854	6669	5174	2659	2141	1058	1387	813	587	307
Occup. Rate (low season) (%)	23	0	0	0	0	0	0	0	0	0	0	0	0
Occup. rate (middle season) (%)	62	64	75	52	64	64	64	64	64	0	64	64	64
Occup. Rate (high season) (%)	86	80	86	84	79	79	79	79	79	79	79	79	79

Fig. 5. Resident and floating population and occupancy rate (%), by municipality, in each touristic season. Source [27].

$$Pfloat_{cs} = (Pres_{cs}/Pres_{Mun}) \; x \; Pfloat_{Mun} \tag{Eq. 4}$$

where: $Pfloat_{cs}$ is the floating population exposure estimated for each census section; $Pres_{cs}$ is the resident population of the census section; $Pres_{Mun}$ is the resident population of the municipality; and $Pfloat_{Mun}$ is the floating population estimated to the municipality by Ref. [31].

The floating population per municipality ($Pfloat_{Mun}$) is the product of the number of tourist beds and the occupancy rate. The two data sources used are: tourist accommodation (number of tourist beds), and tourism supply occupancy (number of occupied tourist beds by number of tourist beds), both extracted from Ref. [27]; based on INE data. This method of estimating floating population is marked with uncertainty arising from calculating that figure through the proportional distribution of municipal floating population to each census section based on their resident population. In fact, occupancy data is not available at that local level of detail.

On each touristic season, the total exposed population results from the sum of the resident population and the floating population estimated for each census section.

The total population exposure was later normalized with the min-max method to the range [0, 1], with 0 being the minimum and 1 the maximum total exposure. To illustrate the data as clearly as possible, the exposed population classes have been divided into the following equal intervals: very low (0–0.20), low (0.20–0.40), moderate (0.40–0.60), high (0.60–0.80) and very high (0.80–1).

3.3. Social vulnerability

3.3.1. Theoretical framework

Social vulnerability (SV) results from the product of two dimensions: criticality (Cr) and support capability (SC) as expressed in Eq. (5) [32];:

$$SV = Cr * (1 - SC) \tag{Eq. 5}$$

According to these authors, social vulnerability is defined from a two-component perspective: criticality and support capability. Criticality groups together the set of intrinsic characteristics of the population living in a territory, such as demographics, education, employment and households, among other variables. Support capability refers to the set of public and private infrastructures, facilities, services and communications networks that support the above-mentioned population. This integrated vision contributes to a more effective and assertive response to adopt protection measures in more vulnerable social groups. It also reinforces resilience to the occurrence of hazardous processes, as it considers the available means of a territory to provide the redundancy of systems, maintain daily routines, and enhance the population's recovery.

Thus, it has been possible to determine which areas of the Tramuntana Range are the most critical and, *a priori*, the most vulnerable social groups to which special or greater attention should be paid in the event of an emergency. These groups are usually elderly people, children, illiterate people, or unemployed people. In the same way, it has been possible to identify areas with a low support capability, i.e., those territories in which there are scarce infrastructures and services to attend.

3.3.2. Data collection and integration

The statistical information concerning the population for the criticality calculation was obtained from the 2011 census of the Spanish Statistics [28] (https://www.ine.es/), and the Balearic Islands Statistics [27], (https://ibestat.caib.es/ibestat/inici). The geo-

graphic information for the calculation of the support capability has been obtained from the online database of Open Street Map available in Geofabrik (https://download.geofabrik.de/europe/spain.html).

While the data sources for the criticality assessment are already expressed at the unit of analysis – the census sections, the data sources for the *SC* assessment are of distinct types (lines, points and polygons) and required its integration to be represented at the census section, computing some statistical indicators.

The multivariate analysis was run separately for each *SV* dimension, which means that two spreadsheets were prepared: one for *Cr* and one for *SC*. Data regarding 34 variables (units: in % of total population) were collected for criticality and data for 15 variables (units: minimum distance, number of facilities within 5 km and density) was gathered for the support capability assessment. For the sake of the article's length efficiency, the name and units of the variables are described only when presenting the results (see section 4.3).

3.3.3. Statistical steps

The Excel files were uploaded in the software SPSS (https://www.ibm.com/es-es/analytics/spss-statistics-software), in order to perform a Principal Component Analysis (PCA). This analysis groups the variables by means of correlation matrices into different Principal Components (also called FACs). Depending on the number of variables, the final model usually returns a range between 3 and 6 FACs for each dimension (*Cr* and *SC*).

By performing PCAs iteratively, pairs of variables with high Pearson Coefficient correlations are eliminated, together with those with low communalities and low loadings in the rotated component matrix. The lower the communalities and the loading on such matrix, the less reliable or the less information a variable provides within the entire data set. Thus, to calculate criticality, the number of variables was reduced from 34 to 10 and 3 FACs were obtained. For the support capability, the final PCA model uses 9 variables from the initial 15, and 3 FACs were obtained. It should be noted that the FACs must group variables from the same thematic areas in order to be valid and a designation is attributed to them according to the thematic area – a key issue demanding the expert interpretation of cardinalities [33–36]. By adding the extracted scores by the method of Bartlett, both criticality and support capability final scores are obtained, and once these have been calculated, Social Vulnerability is obtained using Eq. (4).

Scores of criticality, support capability and social vulnerability are spatially represented in a GIS, where five classes are established according to the standard deviation (SD), as follows: very low (< -1.5 SD), low (−1.5 to −0.5 SD), moderate (−0.5 to 0.5 SD), high (0.5–1.5 SD) and very high (>1.5 SD).

The analysis contributes to observing how and why some variables are correlated with others (P. P. [37], allow to understand in detail the dynamics and characteristics of the population and the infrastructures of each census section.

3.4. Risk

Rockfall risk (*R*) is the product of *H*, *E* and *SV*. Since there are three scenarios of exposed population according to the three tourist seasons, three risk scenarios have also been obtained according to these seasons. Using a GIS, these data are spatially represented on maps, classified in the following risk classes, according to the SD: low (< -0.5 SD), moderate (0.5–0.5 SD), high (0.5–1.5 SD) and very high (>1.5 SD).

4. Results

4.1. Rockfall hazard

The map of simulated rockfall trajectories constitutes the basis for the calculation of the spatial probability or susceptibility to rockfall occurrence, at the census section level (Fig. 3A). In this map, the maximum number of simulated trajectories is 1130, mainly concentrated in the Escorca and Fornalutx municipalities, resulting in a very high spatial susceptibility to rockfall (Fig. 6A). The central municipalities of the region show an overall high susceptibility, while the westernmost municipalities (Andratx, Calvià and Puigpunyent) show the lower susceptibility values. It is noteworthy the internal variability in susceptibility within specific municipalities, like Sóller or Pollença. The internal variability of these municipalities is also observable in the temporal probability of rockfall occurrence, ranging from low to high, although the temporal probability is overall moderate in the whole region (Fig. 6B). The probability of rockfall occurrence based on its magnitude is very high or high in the central municipalities of the region, with the exception of Sóller, where it is low (Fig. 6C). This is also the case for Calvià, as well as most of Andratx and Pollença municipalities.

The rockfall hazard is high or very high in Banyalbufar, Deià, Valdemossa and Fornalutx, together with the easternmost census section of Andratx, in which there is a high variability of hazard classes (Fig. 6D). Hazard is moderate in Escorca, Estellencs and some census section of Andratx, Bunyola and Pollença, while in the remaining territory, hazard is low (Fig. 6D). It is noteworthy the variability of hazard within some municipalities, such as Bunyola, Pollença and especially Andratx.

4.2. Exposure in the three touristic scenarios

The exposure scenarios according to the touristic seasons are mapped in Fig. 7 at the census section level. Since the interval classes are constant across the maps, the levels of exposure are directly comparable. The greatest variations in population between seasons are observed in the municipalities of Andratx, Calvià and Pollença, with the exposed population being higher in the high tourist season (Fig. 7C). As an example, the Calvià and Escorca municipalities are further analyzed.

With 61,678 touristic accommodations, Calvià reaches a floating population of +53,043 people in the high season, June to September (86 % of occupancy rate in hotel units), which contrasts with 23 % in the low season to which corresponds a floating population of +14,186 persons. These numbers are in addition to the resident population of 49,675 inhabitants.
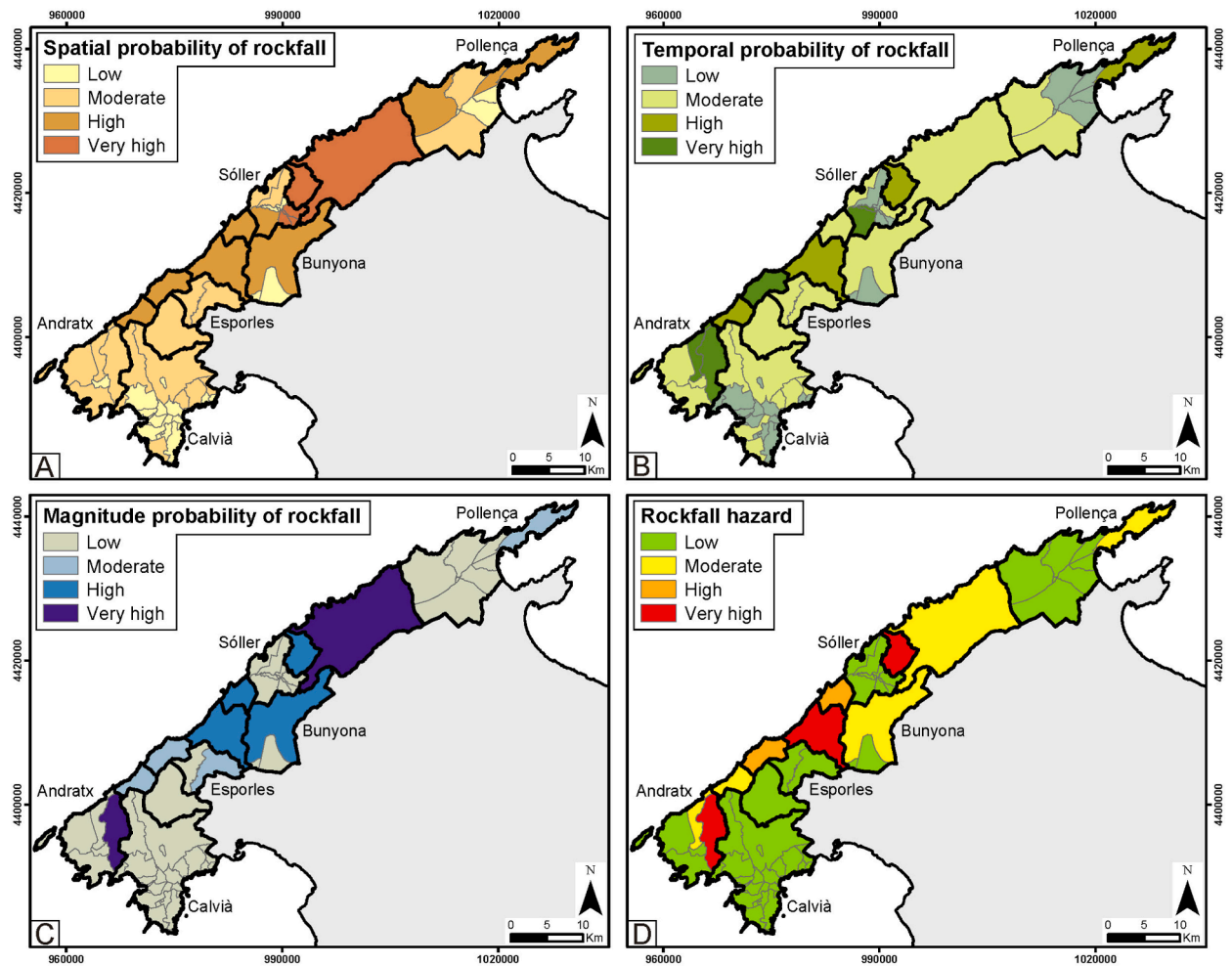
Fig. 6. Spatial probability (A), temporal probability (B), magnitude probability (C) and final hazard map of rockfall occurrence (D) in the Serra de Tramuntana region.

In the opposing spectrum, the Escorca municipality features only 59 touristic accommodations with 0 % occupancy rate in the low season and 79 % in the high season (an increase of 47 persons adding the 260 residents). There are also subtle changes in some census sections in Bunyola and Sóller.

4.3. Social vulnerability

The final PCA model for criticality presented a Kaiser-Meyer-Olkin (KMO) of 0.709, which denotes the very good suitability of the dataset to principal components analysis.

Combining Table 1 data with the maps of Fig. 8, the following interpretation and discussion of criticality is made possible:

- FAC1 - education and age (cf. Fig. 8A). This principal component of criticality presents a common association of elderly people and lower qualifications. The 3 more explicative variables of FAC1 present a positive sign. Surprisingly, there is no correlation between the population over 65 years old and the foreign population, contrasting with the generalized idea that most foreigners are retirees from other countries. Eventually, census data are not capturing the reality of foreign retirees residing in the Tramuntana Range (they are still registered in their countries of origin, paying taxes there, etc.). In fact, foreign population in FAC1 presents a negative loading (−0.421), opposing to the variable expressing elder residents. Note also that positive signs in the two qualification-related variables oppose a negative sign in the variable households with 5 or more residents, usually associated with young families.

- FAC2 – housing conditions (cf. Fig. 8B). New and modern buildings (with elevator and access for persons with disabilities) are strongly associated with the foreign population. Since high percentage of buildings with elevator and disability-friendly express low vulnerability and oppose to areas where buildings need repairs (−0.242 loading), the cardinality is negative and the Bartlett scores of each census section were inverted (multiplied by −1). The three more explicative variables, in blue, lead to infer that foreign population in the Tramuntana Range show good financial condition and good housing conditions, and probably with better academic training.
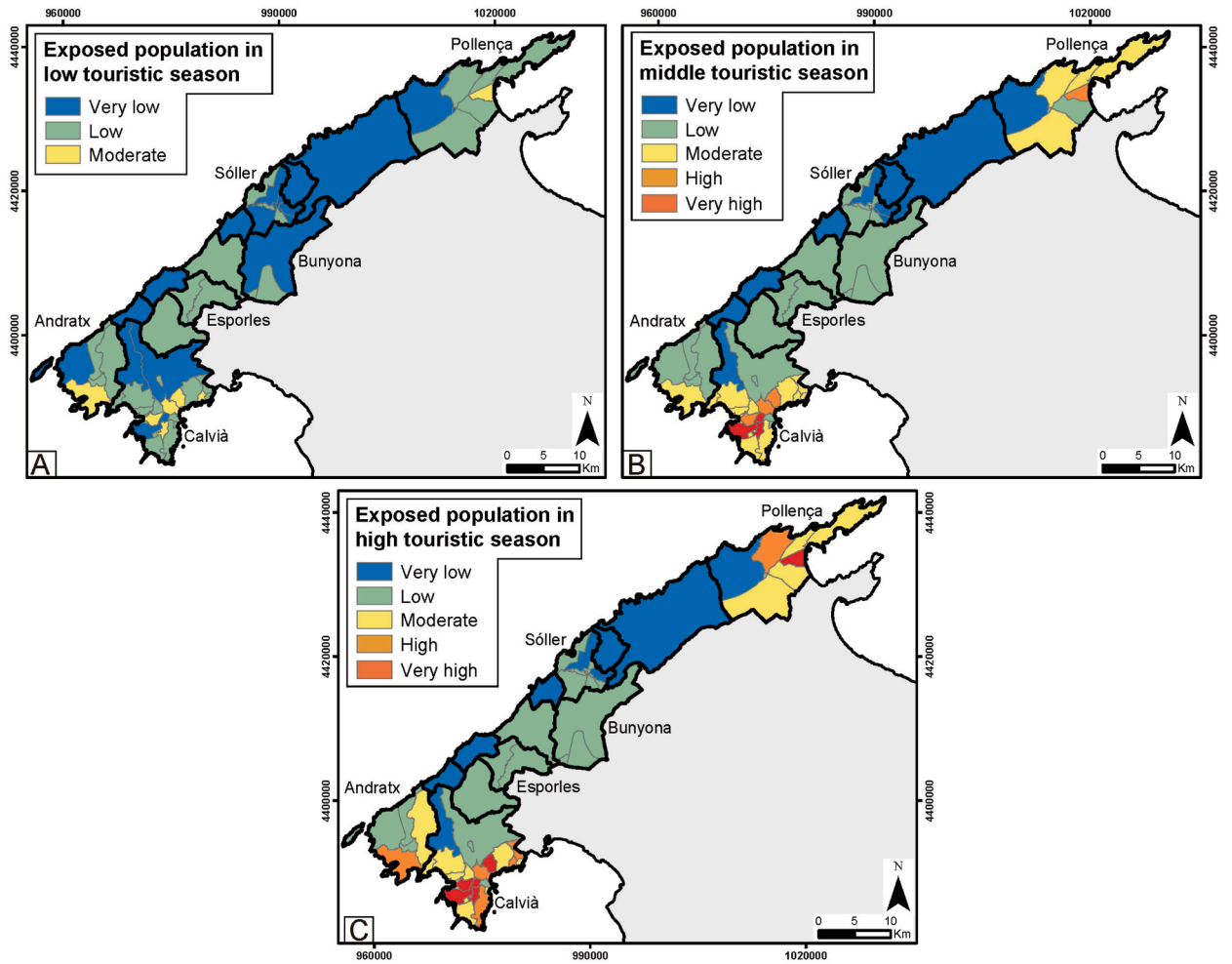
Fig. 7. Exposure of the resident and floating population in the low (A - November, December, January and February), middle (B - March, April, May and October) and high (C - June, July, August and September) touristic seasons.

Table 1
Rotated component matrix for criticality.

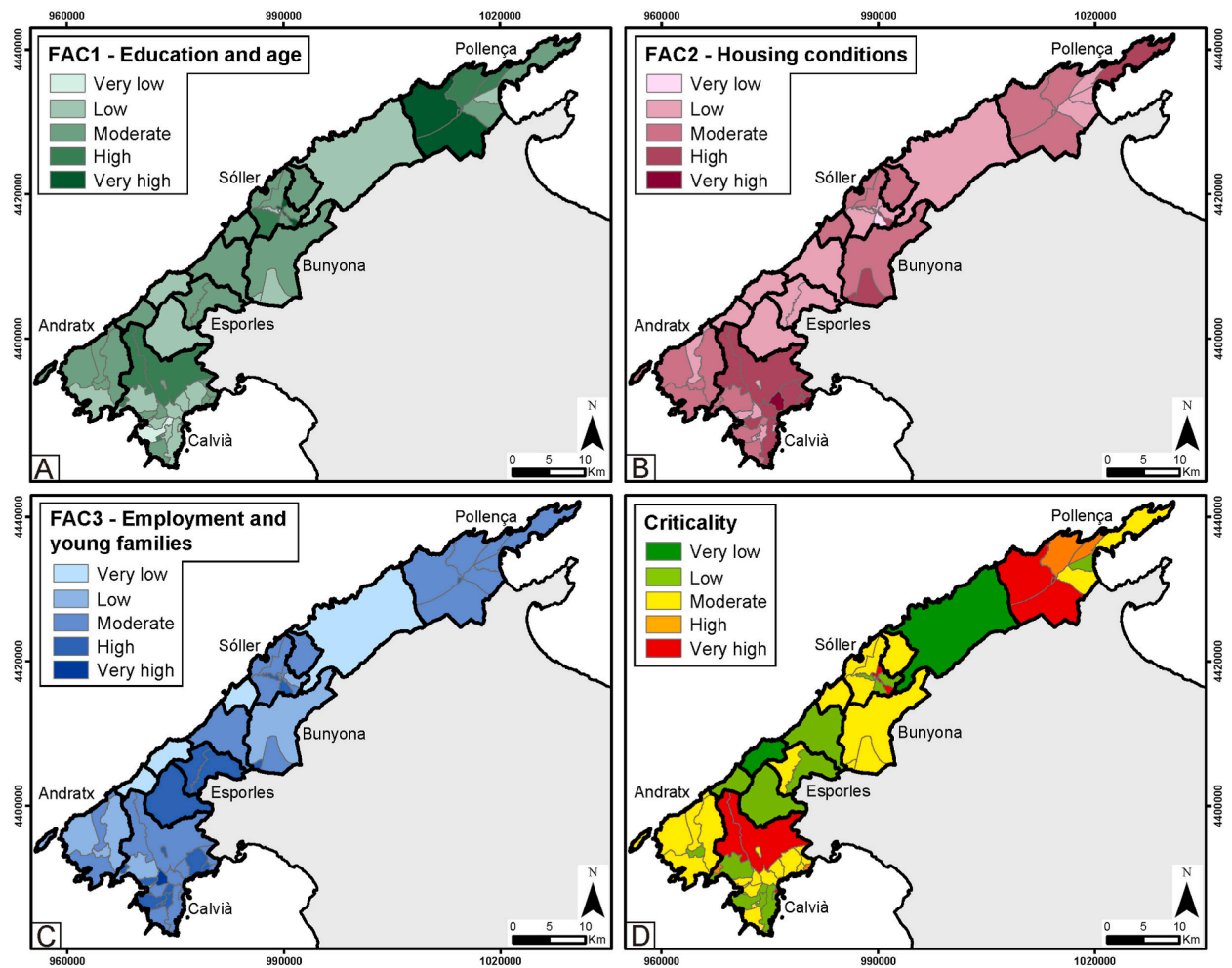|	Criticality principal components (FAC)		
	1	2	3
Illiteracy (%) (pob_sn)	0.778	−0.326	−0.021
Pop. with 1st grade (%) (pob_pr)	0.718	−0.182	−0.042
Pop. with more than 65 years (%) (pob_65)	0.622	−0.253	−0.301
Women population (%) (pob_fem)	0.478	0.353	0.408
Buildings with elevator (ed_asc)	−0.245	0.721	0.054
Buildings disability-friendly (%) (ed_acc)	−0.060	0.709	0.233
Foreign population (%) (pob_ex)	−0.421	0.630	0.056
Employed pop. (%) (pob_emp)	0.011	0.139	0.768
Buildings needing repairs (%) (ed_def)	0.083	−0.242	−0.724
Households with 5 or more residents (hog_5p)	−0.472	−0.303	0.644
Cardinality	+	-	-
% of variance explained	*31.794*	*15.544*	*12.385*
Extraction method: principal component analysis.			
Rotation method: Varimax with Kaiser normalization			
Rotation has converged in 8 iterations.			

Fig. 8. Principal components of criticality (FAC1 - Education and age (A); FAC2 - Housing conditions (B); FAC3 – Employment and young families (C)) and its final expression (D).

- FAC3 – employment and young families (cf. Fig. 8C). Cardinality in this FAC is also negative. High employment rates express mean low vulnerability but the signal of this variable is positive (0.768); on the other hand, buildings needing repairs have a negative loading (−0.724). This means that high Bartlett scores express low vulnerability and justify the multiplication by −1 to express correctly criticality, since PCA is not informed on the theoretical role of variables in regard to criticality. What stands out in FAC3 is the relation between female population and employment rate (both with positive loading), which may be explained due to the employment in the service sector (or tertiary sector), a sector that is mostly occupied by women. Therefore, women would not be a vulnerable group when employed. In addition, housing conditions are probably fair in this population, as the variable buildings needing repairs present an opposing (i.e., negative) loading to the previous variables.

After summing up the scores globally, it emerged that criticality is higher in the northern census sections of Andratx and in the westernmost sections of Pollença, being overall moderate or low in the whole region.

The final PCA model for support capability presented a Kaiser-Meyer-Olkin (KMO) of 0.655, which denotes a fair suitability of the dataset to principal components analysis.

Table 2 allows the interpretation of support capability in the following principal components:.

- FAC1 – Essential infrastructures (cf. Fig. 9A). This component expresses the coverage by grocery stores, pharmacies and health centers in the territory, expressing the existence of essential services and infrastructure, more than emergency ones. Since the lowest the distance, the better the coverage, the Bartlett scores required inversion by multiplication by −1. The highest inverted Bartlett scores are found in the most urbanized and economically dynamic census sections of the municipalities of Deià and Calvià.
- FAC2 – Emergency infrastructures (cf. Fig. 9B). This component has as the most explicative variables, such as the number of temporary shelter facilities (0.824), number of hotels in a radius of 5 km from the block centroid (0.740) and minimum distance to the nearest hospital (0.694), all with a positive sign, which implied using the absolute value of the Bartlett scores because both

Table 2
Rotated component matrix for support capability.

	Support capability principal components (FAC)		
	1	2	3
Min. distance to a grocery store (dmin_ese)	0.925	−0.144	0.010
Min. distance to a pharmacy (dmin_farm)	0.882	−0.149	−0.145
Min. distance to a health centre (dmin_cs)	0.810	0.242	−0.175
No. of temporary shelter facilities within 5 km (temp_5 km)	−0.010	0.824	0.232
No. of hotels within 5 km (nh_5 km)	−0.362	0.740	0.007
Min. distance to a hospital (dmin_hos)	0.435	0.694	−0.072
No. of police stations within 5 km (npol_5 km)	−0.108	0.083	−0.908
No. of gas/electric stations within 5 km (ngas_5 km)	−0.284	0.457	0.737
Road network density (den_carr)	−0.477	0.115	0.641
Cardinality	**-**	**Abs**	**Abs**
% of variance explained	*38.042*	*22.935*	*15.216*

Extraction method: principal component analysis.
Rotation method: Varimax with Kaiser normalization
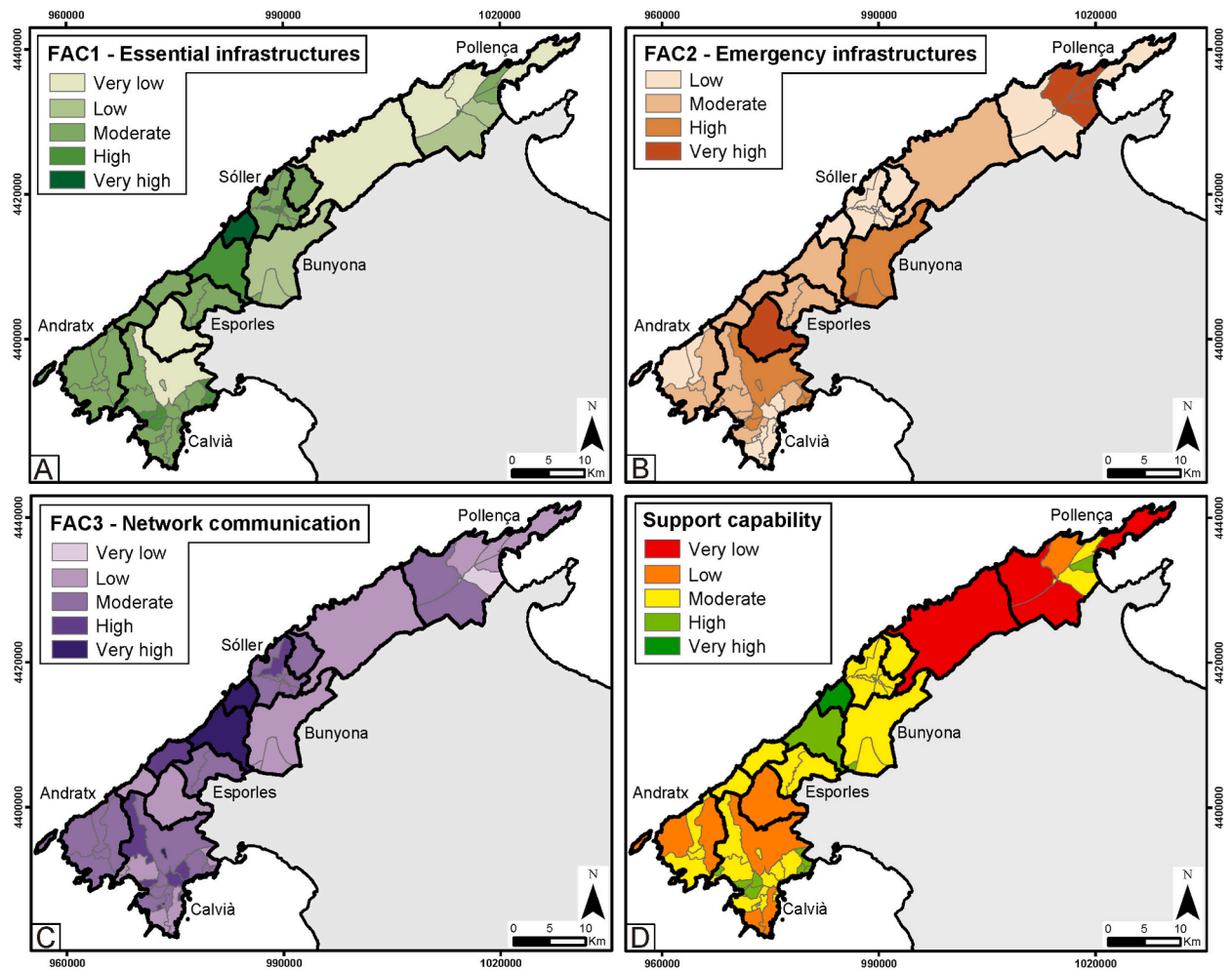Rotation has converged in 8 iterations.

Fig. 9. Principal components of support capability (FAC1 – Essential infrastructures (A); FAC2 – Emergency infrastructures (B); FAC3 – Network communication (C)) and its final expression (D).

extreme scores in this PC mean high coverage (i.e., the highest the number of elements in 5 km the better, and the lowest the minimum distance the better). Using the absolute value (Abs.) is common in vulnerability studies, normally i) in territorial units where both good coverage exists from different facilities according to the method used to represent them, ii) and where contrasting values predominate in different units but both represent high vulnerability, like in the case of age (where both the predominance of children and of elderly persons in different locations are considered vulnerable [33] or urban/rural contrasts [36].

- FAC3 – Network communication (cf. Fig. 9C). The coverage by police stations is the most explicative variable in this principal component. As the PCA is blind to the role of each variable, the Bartlett scores below zero needed to be inverted so a high number of police stations represents high support capability. Only negative values were inverted because the other two strongest variables in FAC3 (number of gas/electric stations within 5 km and road network density) present a correct cardinality in terms of coverage (the highest, the better).

After summing up the scores globally, it is evident that the region generally exhibits a moderate to low level of support capability, with the lowest values observed in the rural and natural areas within the municipalities of Escorca and Pollença (Fig. 9D).

Combining criticality and support capability (Eq. (2)) results in the final mapping of social vulnerability (Fig. 10). There is a considerable variability between and within municipalities. Only the municipality of Escorca has an extremely low social vulnerability, which is the most optimal scenario in case of emergency. Next, the municipalities of Estellencs, Puigpunyent and Banyalbufar have low social vulnerability, along with one census section of Esporles, some southern blocks of Calvià and the easternmost block of Pollença. All the census sections of Andratx and Bunyola, along with several in Calvià, Sóller, Pollença and the municipalities of Valldemossa and Deià have moderate social vulnerability, which is the dominant class in the Tramuntana region. Finally, one census section in the north of Calvià and one in Sóller have high social vulnerability, while another block in the north of Calvià has very high vulnerability along with the two westernmost blocks in Pollença. These territories with high and very high vulnerability classes should be given special attention in the event of an emergency.

4.4. Rockfall risk in the three touristic scenarios

From the product of hazard, exposure in the three touristic seasons and social vulnerability, three final rockfall risk maps were obtained at the census section level for each exposure scenario: low, middle and high (Fig. 11A, B and 11C, respectively). Changes in rockfall risk across the different exposure scenarios are subtle but should not be ignored. The subtleness in risk score differences is due to the attenuation of values caused by the product of scores ranging from 0 to 1, and thus, the significant exposure variations within municipalities become overall smoothed.

Major changes occur in some census sections of Calvià, which change from low to moderate risk from low to middle season, together with the municipality of Escorca, which also changes from low to moderate risk from low to middle season (Fig. 11A and B). No changes were obtained between medium and high season (Fig. 11B and C). Taking the highest risk scenario, in the high tourist season (Fig. 11C), the risk obtained is moderate in most census sections. Very high risk has been obtained in the municipality of Forna-
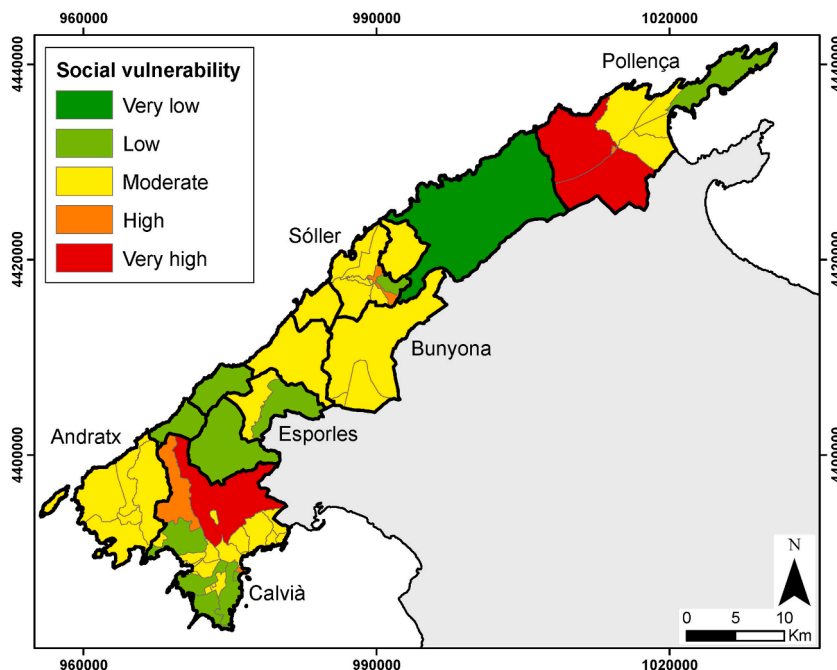

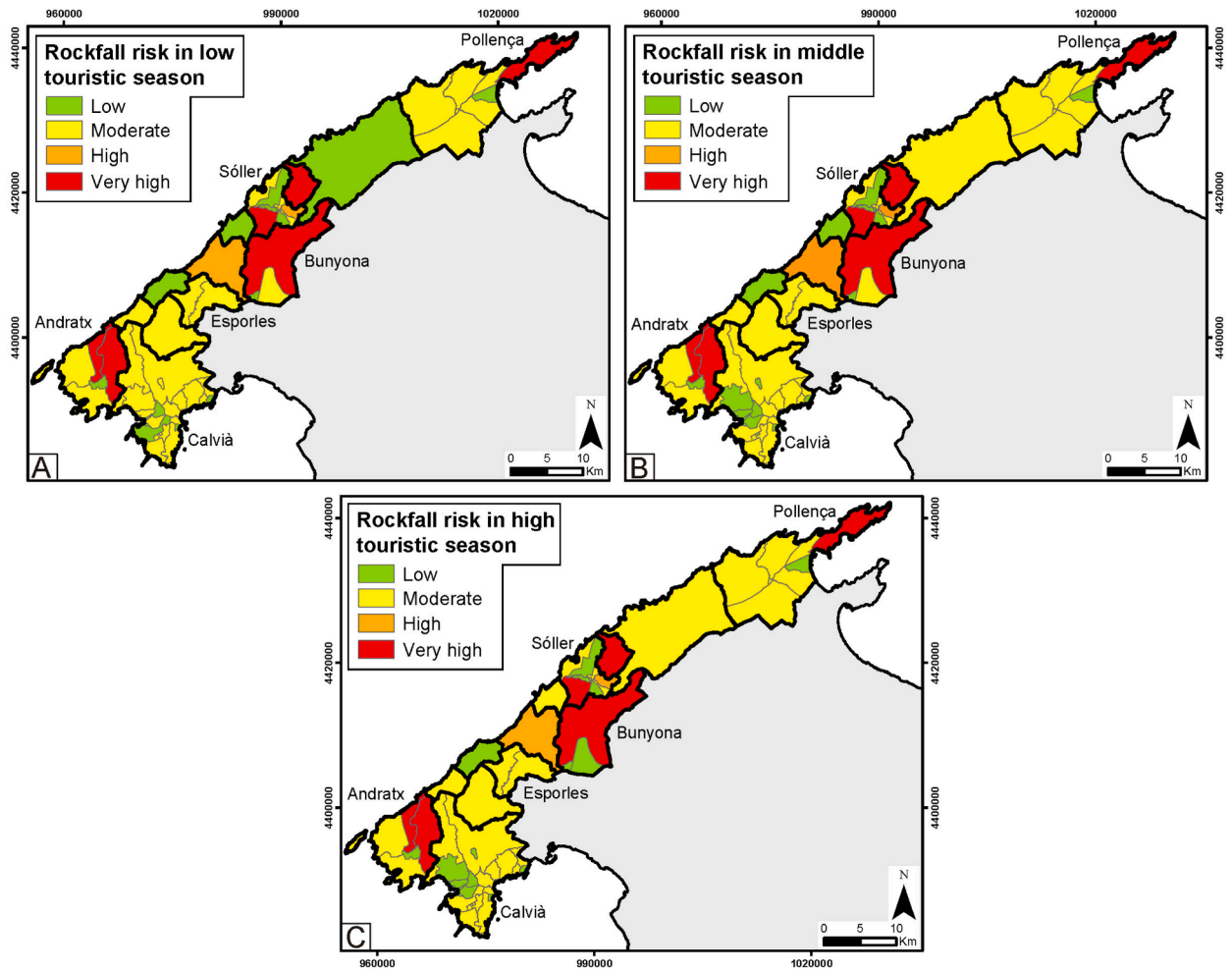**Fig. 10.** Social vulnerability in the Tramuntana Region (Mallorca, Spain).

Fig. 11. Rockfall risk in the Tramuntana Region according to the touristic season: low exposure (A), medium exposure (B) and high exposure (C).

lutx together with the western census sections of Andratx, in one section of Sóller, in the largest section of Bunyola and in the eastern-most one of Pollença. The risk obtained is high in the municipality of Valldemossa, as well as in one census section in Sóller. Finally, the risk obtained is low in the central area of Andratx, the municipality of Banyalbufar, some western areas of Calvià, the southern part of Bunyola and the central census sections of Sóller. It is worth highlighting the variability of risk that exists within some munici-palities, such as Andratx, Bunyola, Sóller and Pollença.

5. Discussion

5.1. Understanding rockfall risk and its components in the Serra de Tramuntana

Rockfall risk analysis, of the nature and detail adopted in this study, aims to emphasize its benefits and utility for civil protection and *trans*-sectorial risk governance entities, both in the public and private sectors. In this way, the frequent slow transfer of scientific knowledge to policy-driven risk mitigation (e.g. Komendantova et al., 2014 [48]) intends to be improved by providing accessible and user-friendly maps. The applicability of this type of analysis arises from the range and significance of the type of input data used and the respective scale at which they were collected, processed, and represented, to produce the final rockfall risk index. In our study case, despite there was some limitations regarding the amount (e.g. temporal and magnitude information of rockfall events) and scale (e.g. floating population at municipality scale) of collected data, we could offer the first rockfall risk analysis of the whole Serra de Tramuntana region, from an acceptable integral approach that combined hazard, social vulnerability and seasonal exposure (Fig. 11). Moreover, it is noteworthy to mention that many of the produced maps (Figs. 4A, 5-11) were utilized in a crisis simulation exercise in April 2022 in Mallorca, successfully achieving the purpose of testing their utility for civil protection stakeholders.

Regarding the hazard, rockfall modelling played an essential role in its calculation, which is already demonstrated to be a power-ful tool for estimating susceptibility (e.g., Ref. [38]. The information gathered in the updated rockfall inventory at regional scale is also of great significance, with no precedents in other study cases in Spain. The compilation of this inventory was primarily made pos-sible thanks to the data provided by the General Directorate of Emergencies of the Government of the Balearic Islands and the Council

Road Service of the Island of Mallorca, data that is not typically readily available. Nevertheless, it should be noted that there is a lack of information regarding the temporal occurrence and magnitude of the rockfall records for many events: only 43.5 % and 19.4 % of the total events were registered with information of date and magnitude, respectively. This must be considered when using the inventory for hazard calculations, namely regarding the temporal probability and magnitude, as this information bias exists. Moreover, as hazard is the product of the spatial, temporal and magnitude probabilities, there are some particular cases where the final hazard score may not align with the initial expectations, what is also conditioned by the selected thresholds of the hazard classes. As an example, the southwestern census section of Sóller shows high or very high temporal and spatial probabilities but a low magnitude probability, what results in a low hazard (Fig. 6). In this case, the final hazard value is 0.212, which is very close to the threshold between the low and moderate hazard classes (i.e., 0.219). Another example is the municipality of Escorca, that shows very high spatial and temporal probabilities and a moderate temporal probability to result in a moderate hazard value (0.44), which is very close to the threshold between the moderate and high hazard classes (0.45).

On the exposure assessment, a noteworthy innovation of this type of study is the consideration of the exposed population across the three distinct tourist seasons, accounting for both permanent residents and temporary visitors. Analyzing this seasonality in tourism, in conjunction with the seasonality of rockfalls, has provided valuable insights into this natural phenomenon within the study region. It is well-documented that rockfalls in the Serra de Tramuntana are notably more frequent during the winter months [50], which coincide with the low tourist season. This observation is further affirmed by our updated inventory, which reveals that 52 % of rockfall events with known dates (Fig. 4B) occurred during the low season, in contrast to 27 % and 21 % during the middle and high seasons, respectively. Similarly, among rockfall events exceeding 600 m^3 in magnitude, 67 % took place during the low tourist season, with 20 % and 13 % occurring during the middle and high seasons, respectively. As an example, the Gorg Blau rockfall in Escorca (30,000 m^3), which occurred in December and blocked the main road of the region (Ma-10), cut off access to one of the most touristy destinations in Mallorca (Sa Calobra cove) [9]. Although the indirect costs amounted to as much as 1 million Euro, they would have been even higher if the incident had taken place during the high tourist season. However, it is worth noting that the event with the highest magnitude (200,000 m^3) occurred in the easternmost census section of Pollença (Cap de Formentor) (Fig. 4C) in September, which corresponds to the high tourist season, and resulted in one fatality [22]. This serves as an illustrative example that, while not common, high-risk events can also occur during the less expected seasons.

Despite its basis on official and directly quantified statistical data, social vulnerability remains a complex risk dimension to be measured, particularly at the detailed scale provided by census sections. Quite often, such analysis is performed at the country, region, district or municipality level [35,39–42]. The relevance of social vulnerability estimations in risk characterization processes is also emphasized by the fact that both criticality and support capability are independent of hazard. This means they provide an insight into the propensity to suffer damage that is not covered by the other risk components. Individual and territorial variables that control social vulnerability are frequently not available from official statistics, and this gap becomes more evident as the level of detail increases [32,34,43–45]. In practice, this can result in an underestimation or concealment of vulnerability drivers within each context.

The final results on risk show certain interesting aspects derived from the combination of hazard, exposure and social vulnerability. One example is the case of Calvià, where, despite having the largest exposed population, the hazard is low and so the resulting risk is moderate. The variability of social vulnerability between the northern and southern census sections of the municipality is also striking. Another interesting example is that of the municipality of Escorca, where the hazard is very high but the social vulnerability and exposed population is in both cases very low, and the risk is finally moderate. Some hotspot rockfall risk areas were evidenced, which was only made possible by considering the different census sections within the municipalities, as a great variability of risk levels has been obtained within them. Some examples of this internal variability can be seen in Andratx, Bunyola, Sóller and Pollença. Therefore, we consider that it is valuable to design emergency plans not only at municipality scale, but also considering the internal peculiarities and variations of each municipality.

Indeed, there are additional risk factors that can significantly influence rockfall risk, including the rise in population density and substantial urban and infrastructure development, notably evident along the coast of Southwest Europe in recent decades [51]. This phenomenon can be attributed to the exponential growth of tourism, resulting in an increased exposure and social vulnerability. Therefore, it is reasonable these risk components may have escalated in the analyzed area since our study relied on census data from 2011.

5.2. Implications for risk management and future strategies

A critical aspect demanding attention is the tourists' often limited awareness of the local environment and its associated hazards, as well as their knowledge of self-protective measures. Tourism serves as a significant driver for socioeconomic development, but it also introduces stress factors by amplifying population exposure to areas with very high and high hazards. This situation poses challenges in terms of risk perception, language barriers, risk communication, and risk management strategies, necessitating a consideration of hazard reduction, exposure reduction, and the mitigation of social vulnerability [12].

Individuals in developed countries often delegate the responsibility for activating protective measures to authorities and the market [52]. This delegation reduces individual proactive conduct and stimulates a paradoxical increase in the levels of sensitivity [46]. Exposure to natural disaster hazards plays a significant role in shaping the connection between economic losses and wealth. Therefore, disaster risk reduction strategies are a priority from this perspective, what creates the need for safety campaigns, both for residents and tourists because Mallorca is an important holidays resort in Europe [29,47]. This creates issues surrounding the safety of tourists in the event of a disaster but also questions how early warning systems and hazard information at a local level can be tailored to best inform and meet the needs of this vulnerable population.

This study aims to highlight the significance of disaster risk management in tourist destinations and the necessity of adopting proactive rockfall risk mitigation strategies (prevention, preparedness, response, and recovery) to reduce risks effectively. Moreover, our work underscores the challenge of precisely representing exposure and vulnerability, specifically, the monitoring of fine-scale variations in seasonal exposure. In this study case, we relied on information about the floating population at the municipalities scale and subsequently recalculated it to the level of census sections. This adjustment was necessary by the absence of raw data at the census section scale, which, in any case, appears unlikely to be obtainable. Therefore, accurately addressing the social vulnerability of temporary visitors adds an additional layer of complexity to this scenario, which is equally as crucial as monitoring and analyzing hazards. Finally, it should be mentioned that, despite the extensive geographic detail in this study, it cannot replace analyses of vulnerability and exposure at the individual building level, where the contribution of georeferenced census data is essential.

6. Conclusions

In addition to the scientific perspective, the aim of the assessment presented in this paper was to provide user-friendly mapping and scenarios of rockfall risk, targeting civil protection agencies and related organizations. This research presents the first comprehensive and highly detailed risk assessment for a geomorphological process in the Serra de Tramuntana region (Mallorca). Among the three commonly used risk components, rockfall hazard and exposure were represented at a high resolution, relying on inventory-based validated data. The evaluation of susceptibility could be greatly improved over this region thanks to the production of a detailed rockfall inventory, as well as to the modelling of rockfall trajectories. Regarding exposure, the inclusion of touristic-related activity enabled us to distinguish three seasonal exposure scenarios, that is a critical consideration in regions characterized by fluctuating populations. This, in turn, resulted in three distinct risk assessments. As for the data used to assess social vulnerability, it was based on the census section level, which provided a remarkably detailed basis for estimating this complex aspect of risk in regional-scale studies. The use of infra-municipal census data allowed for the identification of some unexpected internal variations – both in the final SV scores as among the support capability and criticality main drivers – within and between municipalities, that otherwise would have gone unnoticed. Ultimately, this study underscored the primary role of census data in territorial and sociodemographic characterization. Despite the positive aspects highlighted, there are still some gaps and limitations in the assessment conducted. Exposure indicators related to the actual presence of floating population still require a more in-depth spatial representation, considering the simultaneously widespread and localized nature of rockfall-prone areas and those areas where trajectories occur. Future evaluations should be undertaken with updated census data, especially regarding exposure and vulnerability considerations. Future evaluations are necessary considering new census data, which is particularly relevant regarding exposure and vulnerability.

CRediT authorship contribution statement

Pedro Pinto Santos: Conceptualization, Data curation, Formal analysis, Investigation, Methodology, Resources, Supervision, Validation, Visualization, Writing – original draft, Writing – review & editing. **Cristina Reyes-Carmona:** Conceptualization, Data curation, Formal analysis, Investigation, Methodology, Project administration, Resources, Validation, Visualization, Writing – original draft, Writing – review & editing. **Susana Pereira:** Conceptualization, Data curation, Formal analysis, Investigation, Methodology, Resources, Supervision, Validation, Visualization, Writing – original draft, Writing – review & editing. **Roberto Sarro:** Data curation, Formal analysis, Funding acquisition, Investigation, Project administration, Supervision, Validation, Visualization, Writing – original draft, Writing – review & editing. **Mónica Martínez-Corbella:** Formal analysis, Investigation, Project administration, Resources, Validation, Visualization, Writing – review & editing. **Miquel Àngel Coll-Ramis:** Data curation, Formal analysis, Investigation, Methodology, Validation, Visualization, Writing – review & editing. **José Luís Zêzere:** Conceptualization, Formal analysis, Funding acquisition, Investigation, Project administration, Resources, Supervision, Validation, Visualization, Writing – review & editing. **Rosa María Mateos:** Conceptualization, Formal analysis, Funding acquisition, Investigation, Methodology, Project administration, Resources, Supervision, Validation, Visualization, Writing – review & editing.

Declaration of competing interest

The authors declare the following financial interests/personal relationships which may be considered as potential competing interests: Pedro Pinto Santos reports financial support was provided by Fundação para a Ciência e a Tecnologia.

Data availability

Data will be made available on request.

Acknowledgments

Appendix A. Supplementary data

Supplementary data to this article can be found online at https://doi.org/10.1016/j.ijdrr.2024.104264.

References

[1] J. Rosselló, S. Becken, M. Santana-Gallego, The effects of natural disasters on international tourism: a global analysis, Tourism Manag. 79 (2020) 104080, https://doi.org/10.1016/J.TOURMAN.2020.104080.

[2] W.Q. Ruan, Y.Q. Li, C.H.S. Liu, Measuring tourism risk impacts on destination image, Sustainability 9 (9) (2017) 1501, https://doi.org/10.3390/SU9091501.

[3] S. Becken, R. Mahon, H.G. Rennie, A. Shakeela, The tourism disaster vulnerability framework: an application to tourism in small island destinations, Nat. Hazards 71 (1) (2014) 955–972, https://doi.org/10.1007/S11069-013-0946-X/TABLES/4.

[4] H.L. Ghimire, Disaster management and post-quake impact on tourism in Nepal, Gaze: J. Tourism Hospit. 7 (2015) 37–57, https://doi.org/10.3126/GAZE.V7I0.15119.

[5] C. Orchiston, J.E.S. Higham, Knowledge management and tourism recovery (de)marketing: the Christchurch earthquakes 2010–2011, Curr. Issues Tourism 19 (1) (2014) 64–84, https://doi.org/10.1080/13683500.2014.990424.

[6] R.M. Mateos, J. López-Vinielles, E. Poyiadji, D. Tsagkas, M. Sheehy, K. Hadjicharalambous, P. Liscák, L. Podolski, I. Laskowicz, C. Iadanza, C. Gauert, S. Todorović, M.J. Auflič, R. Maftei, R.L. Hermanns, A. Kociu, C. Sandić, R. Mauter, R. Sarro, G. Herrera, Integration of landslide hazard into urban planning across Europe, Landsc. Urban Plann. 196 (2020) 103740, https://doi.org/10.1016/J.LANDURBPLAN.2019.103740.

[7] D.J. Varnes, Slope movement types and processes, in: R.L. Schuster, R.J. Krizek (Eds.), Landslides, Analysis and Control, vol. 176, Transportation Research Board Special Report, 1978, pp. 11–33.

[8] R. Sarro, R.M. Mateos, I. García-Moreno, G. Herrera, P. Reichenbach, L. Laín, C. Paredes, The Son Poc rockfall (Mallorca, Spain) on the 6th of March 2013: 3D simulation, Landslides 11 (3) (2014) 493–503, https://doi.org/10.1007/s10346-014-0487-8.

[9] R.M. Mateos, I. García-Moreno, P. Reichenbach, G. Herrera, R. Sarro, J. Rius, R. Aguiló, F. Fiorucci, Calibration and validation of rockfall modelling at regional scale: application along a roadway in Mallorca (Spain) and organization of its management, Landslides 13 (4) (2016) 751–763, https://doi.org/10.1007/s10346-015-0602-5.

[10] L.Q. de Almeida, T. Welle, J. Birkmann, Disaster risk indicators in Brazil: a proposal based on the world risk index, Int. J. Disaster Risk Reduc. 17 (2016) 251–272, https://doi.org/10.1016/j.ijdrr.2016.04.007.

[11] U. Deichmann, D. Ehrlich, C. Small, G. Zeug, Using high resolution satellite data for the identification of urban natural disaster risk, in: European Union and World Bank, 2011.

[12] S. Pereira, P.P. Santos, J.L. Zêzere, A.O. Tavares, R.A.C. Garcia, S.C. Oliveira, A landslide risk index for municipal land use planning in Portugal, Sci. Total Environ. 735 (2020) 139463, https://doi.org/10.1016/j.scitotenv.2020.139463.

[13] I. Schumacher, E. Strobl, Economic development and losses due to natural disasters: the role of hazard exposure, Ecol. Econ. 72 (2011) 97–105, https://doi.org/10.1016/j.ecolecon.2011.09.002.

[14] V. Kennedy, K.R. Crawford, G. Main, R. Gauci, J.A. Schembri, Stakeholder's (natural) hazard awareness and vulnerability of small island tourism destinations: a case study of Malta, Tour. Recreat. Res. 47 (2) (2020) 160–176 https://doi.org/10.1080/02508281.2020.1828554, 2020.1828554.

[15] D.N. Nguyen, F. Imamura, K. Iuchi, Public-private collaboration for disaster risk management: a case study of hotels in Matsushima, Japan, Tourism Manag. 61 (2017) 129–140, https://doi.org/10.1016/J.TOURMAN.2017.02.003.

[16] M. Ruiz-Pérez, M. Gelabert Grimalt, Análisis de la Vulnerabilidad Social Frente a Desastres Naturales: el Caso de la Isla De Mallorca, Geografía y Sistemas de Información Geográfica, 2012, pp. 1–26. http://www.gesig-proeg.com.ar/documentos/revista-geosig/2012/Investigacion/01-RUIZ-GRIMALT-GOESIG4-2012.pdf.

[17] X. Wang, P. Frattini, G.B. Crosta, G.B. Crosta, L. Zhang, F. Agliardi, S. Lari, Z. Yang, Uncertainty assessment in quantitative rockfall risk assessment, Landslides 11 (2014) 711–722, https://doi.org/10.1007/s10346-013-0447-8.

[18] G. Torsello, G. Vallero, L. Milan, M. Barbero, M. Castelli, A quick QGIS-based procedure to preliminarily define time-independent rockfall risk: the case study of Sorba Valley, Italy, Geosciences 12 (2022) 305, https://doi.org/10.3390/geosciences12080305.

[19] M. Castelli, C. Scavia, A multidisciplinary methodology for hazard and risk, assessment of rock avalanches, Rock Mech. Rock Eng. 41 (1) (2008) 3–36, https://doi.org/10.1007/s00603-007-0151-x.

[20] M. Papathoma-Köhle, M. Schlögl, S. Fuchs, Vulnerability indicators for natural hazards: an innovative selection and weighting approach, Sci. Rep. 9 (2019) 15026, https://doi.org/10.1038/s41598-019-50257-2.

[21] R.M. Mateos, P. Ezquerro, J.M. Azañón, B. Gelabert, G. Herrera, J.A. Fernández-Merodo, D. Spizzichino, R. Sarro, I. García-Moreno, M. Béjar-Pizarro, Coastal lateral spreading in the world heritage site of the Tramuntana Range (Majorca, Spain). The use of PSInSAR monitoring to identify vulnerability, Landslides 15 (4) (2018) 797–809, https://doi.org/10.1007/s10346-018-0949-5.

[22] R.M. Mateos, Los movimientos de ladera en la Serra de Tramuntana (Mallorca), Caracterización geomecánica y análisis de peligrosidad [Universidad Complutense de Madrid, 2006. https://produccioncientifica.ucm.es/documentos/5d1df60c29995204f765fbfb.

[23] M. Ferrer, J.M. López, R.M. Mateos, R. Morales, A. Rodríguez-Perea, Análisis de los Desprendimientos Rocosos en la Cala de Banyalbufar. Boletín Geológico y Minero, Marzo–Abril de, 1997, pp. 39–51 1997.

[24] R.M. Mateos, J.M. Azañón, Los movimientos de ladera en la Sierra de Tramuntana de la Isla de Mallorca: tipos, características y factores condicionantes, Rev. Soc. Geol. Espana 18 (1–2) (2005) 89–99.

[25] R.M. Mateos, I. García-Moreno, G. Herrera, J. Mulas, Losses caused by recent mass-movements in Majorca (Spain), Landslide Sci. Practice: Soc. Econ. Impact Pol. 7 (October) (2013) 105–111, https://doi.org/10.1007/978-3-642-31313-4_14.

[26] R.M. Mateos, I. García-Moreno, G. Herrera, J. Mulas, in: C. Margottini, P. Canuti, K. Sassa (Eds.), Recent Mass Movements in the Tramuntana Range (Mallorca, Spain). Landslide Science and Practice, Global Environmental Change, ume 4, Springer, 2013, pp. 27–37.

[27] B.I.S. Ibestat, FRONTUR: touristic statistical data, https://ibestat.caib.es/ibestat/estadistiques/043d7774-cd6c-4363-929a-703aaa0cb9e0/3f1887a5-b9b7-413b-9159-cb499cf29246/es/I208002_n301.px, 2022.

[28] S.S. Ine, 2011 population census, https://www.ine.es/, 2011.

[29] M. Grimalt-Gelabert, J. Rosselló-Geli, J. Bauzà-Llinàs, Flood related mortality in a touristic island: Mallorca (Balearic Islands) 1960–2018, J. Flood Risk Manag. 13 (4) (2020) e12644, https://doi.org/10.1111/JFR3.12644.

[30] F. Guzzetti, G. Crosta, R. Detti, F. Agliardi, STONE: a computer program for the three-dimensional simulation of rock-falls, Comput. Geosci. 28 (9) (2002) 1079–1093, https://doi.org/10.1016/S0098-3004(02)00025-0.

[31] M.À. Coll-Ramis, Análisis Socio-espacial de la Estacionalidad Turística en Mallorca, 2016.

[32] J.M. Mendes, A.O. Tavares, P.P. Santos, Social vulnerability and local level assessments: a new approach for planning, Int. J. Disaster Resil. Built Environ. 11 (1) (2019) 15–43, https://doi.org/10.1108/IJDRBE-10-2019-0069.

[33] S.L. Cutter, B.J. Boruff, W.L. Shirley, Social vulnerability to environmental hazards, Soc. Sci. Q. 84 (2) (2003) 242–261, https://doi.org/10.1111/1540-6237.8402002.

[34] M.C. Schmidtlein, R.C. Deutsch, W.W. Piegorsch, S.L. Cutter, A sensitivity analysis of the social vulnerability index, Risk Anal. 28 (4) (2008) 1099–1114, https://doi.org/10.1111/j.1539-6924.2008.01072.x.

[35] A.O. Tavares, J.L. Barros, J.M. Mendes, P.P. Santos, S. Pereira, Decennial comparison of changes in social vulnerability: a municipal analysis in support of risk management, Int. J. Disaster Risk Reduc. 31 (2018) 679–690, https://doi.org/10.1016/j.ijdrr.2018.07.009.

[36] Y. Zhou, N. Li, W. Wu, J. Wu, P. Shi, Local spatial and temporal factors influencing population and societal vulnerability to natural disasters, Risk Anal. 34 (4) (2014) 614–639, https://doi.org/10.1111/risa.12193.

[37] P.P. Santos, J.L. Zêzere, S. Pereira, J. Rocha, A.O. Tavares, A novel approach to measuring spatiotemporal changes in social vulnerability at the local level in Portugal, Int. J. Disaster Risk Sci. 13 (6) (2022) 842–861, https://doi.org/10.1007/s13753-022-00455-w.

[38] M. Alvioli, M. Santangelo, F. Fiorucci, M. Cardinali, I. Marchesini, P. Reichenbach, M. Rossi, F. Guzzetti, S. Peruccacci, Rockfall susceptibility and network-ranked susceptibility along the Italian railway, Eng. Geol. 293 (2021) 106301, https://doi.org/10.1016/j.enggeo.2021.106301.

[39] W. Chen, S.L. Cutter, C.T. Emrich, P. Shi, Measuring social vulnerability to natural hazards in the Yangtze River Delta region, China, Int. J. Disaster Risk Sci. 4 (4)

(2013) 169–181, https://doi.org/10.1007/s13753-013-0018-6.

[40] S.L. Cutter, C. Finch, Temporal and spatial changes in social vulnerability to natural hazards, Plan. Clim. Change: Read. Green Infrastruct. Sustain. Des. Resil. Cities 105 (7) (2018) 129–137, https://doi.org/10.4324/9781351201117-16.

[41] G. Park, Z. Xu, Spatial and temporal dynamics of social vulnerability in the United States from 1970 to 2010: a county trajectory analysis, Int. J. Appl. Geospatial Res. (IJAGR) 11 (1) (2020) 19, https://doi.org/10.4018/IJAGR.2020010103.

[42] D.K. Yoon, Assessment of social vulnerability to natural disasters: a comparative study, Nat. Hazards 63 (2) (2012) 823–843, https://doi.org/10.1007/s11069-012-0189-2.

[43] S. Rufat, E. Tate, C.G. Burton, A.S. Maroof, Social vulnerability to floods: review of case studies and implications for measurement, Int. J. Disaster Risk Reduc. 14 (2015) 470–486, https://doi.org/10.1016/j.ijdrr.2015.09.013.

[44] P.P. Santos, A. Tavares, P. Freire, A. Fortunato, A. Rilo, Territorial vulnerability to flooding in an estuarine area: challenges valuing the structural and societal local ensemble, Saf. Reliab. Compl. Eng. Syst. (2015) 4273–4280, https://doi.org/10.1201/b19094-560.

[45] A.O. Tavares, P.P. Santos, P. Freire, A.B. Fortunato, A. Rilo, L. Sá, Flooding hazard in the Tagus estuarine area: the challenge of scale in vulnerability assessments, Environ. Sci. Pol. 51 (2015) 238–255, https://doi.org/10.1016/j.envsci.2015.04.010.

[46] I. Schumacher, E. Strobl, Economic development and losses due to natural disasters: the role of hazard exposure, Ecol. Econ. 72 (2011) 97–105, https://doi.org/10.1016/J.ECOLECON.2011.09.002.

[47] M. Gasc-Barbier, R.M. Mateos, C. Lasio, A. Villatte, S. Bernardie, C. Reyes-Carmona, R. Sarro, M. Martínez-Corbella, J.A. Luque, J. López-Vinielles, O. Monserrat, Crisis exercise in the framework of coastal geohazards: experience in the Balearic Islands (Spain). Int. J. Disaster Risk Reduc. (under review).

[48] N. Komendantova, R. Mrzyglocki, A. Mignan, B. Khazai, F. Wenzel, P. Anthony, K. Fleming, Multi-hazard and multi-risk decision-support tools as a part of participatory risk governance: feedback from civil protection stakeholders, Int. J. Disaster Risk Reduc. 8 (2014) 50–67, https://doi.org/10.1016/j.ijdrr.2013.12.006.

[49] F. Sàbat, B. Gelabert, A. Rodríguez-Perea, J. Giménez, Geological structure and evolution of Majorca: implications for the origin of the Western Mediterranean, Tectonophysics 510 (2011) 217–238, https://doi.org/10.1016/j.tecto.2011.07.005.

[50] R.M. Mateos, I. García-Moreno, J.M. Azañón, Freeze–thaw cycles and rainfall as triggering factors of mass movements in a warm Mediterranean region: the case of the Tramuntana Range (Majorca, Spain), Landslides 9 (2012) 417–432, https://doi.org/10.1007/s10346-011-0290-8.

[51] R.M. Mateos, R. Sarro, A. Díez-Herrero, C. Reyes-Carmona, J. López-Vinielles, P. Ezquerro, M. Martínez-Corbella, G. Bru, J.A. Luque, A. Barra, et al., Assessment of the socio-economic impacts of extreme weather events on the coast of southwest Europe during the period 2009–2020, Appl. Sci. 13 (2023) 2640, https://doi.org/10.3390/app13042640.

[52] P.A. Raschky, H. Weck-Hannemann, Charity hazard—a real hazard to natural disaster insurance? Environ. Hazards 7 (4) (2007) 321–329, https://doi.org/10.1016/j.envhaz.2007.09.002.